Photophysical properties of solid films of fullerene, C_{60}

1991 J. Phys.: Condens. Matter 3 9259

(http://iopscience.iop.org/0953-8984/3/47/001)

J. Phys.: Condens. Matter 3 (1991) 9259–9270. Printed in the UK

Photophysical properties of solid films of fullerene, C_{60}

K Pichler†, S Graham†, O M Gelsen†, R H Friend†, W J Romanow‡, J P McCauley Jr‡§, N Coustel‡‖, J E Fischer‡‖ and A B Smith III‡§

† Cavendish Laboratory, Madingley Road, Cambridge CB3 0HE, UK

‡ Laboratory for Research on the Structure of Matter, University of Pennsylvania, Philadelphia, PA 19104-6272, USA

Received 12 September 1991

Abstract. We report results on photophysical properties of solid films of C_{60}, including optical absorption, photoluminescence, electroabsorption, photoconductivity, and photoinduced absorption. We observe photoconductivity for excitation energies from the UV to the near IR and find that the excitation spectrum follows the optical absorption. The electroabsorption response varies quadratically with electric field, shows oscillations at the band edge, and has an anisotropy of slightly less than three with respect to the light polarization and the direction of the applied electric field. Photoluminescence from excited states shows vibrational fine structure, a strong temperature dependence, and some variation with excitation energy. We see photoinduced absorption attributed to triplet–triplet transitions at 1.7 eV and also a band peaking at 1.3 eV. A further band at 2.33 eV is seen in C_{60}/C_{70} mixtures (10% C_{70}) and also in degraded C_{60} samples. We consider that these bands may arise from extrinsic stabilization of photo-separated charges.

1. Introduction

Shell-structured carbon molecules, in particular C_{60} (Buckminsterfullerene, fullerene, etc), have raised considerable interest recently, partly because they may provide the resolution to the identification of spectra from interstellar space [1–3]. Since the fullerenes became available in quantity [4, 5], a great deal of experimental work on C_{60} has been carried out and these materials are now known to show superconductivity at high temperatures when doped with alkali metals [6, 7].

The icosahedral C_{60} molecule has a closed-shell structure with the surface consisting of twelve-, five- and twenty-six-membered carbon rings with bond length alternation on the six-membered rings. The structure of C_{60} (and other carbon clusters) and its aromaticity have been convincingly demonstrated, and agreement between theory and experiment (IR, Raman, NMR, ESCA, X-ray diffraction, and others) is generally good, at least with respect to the geometrical structure [8]. The presence of the extended valence electron system provides an interesting experimental system for the study of electronic excitations, and there are interesting comparisons to make with conjugated molecules such as polyacetylene and other conjugated polymers.

§ Also at: Chemistry Department, University of Pennsylvania, Philadelphia, PA 19104-6272, USA.

‖ Also at: Materials Science Department, University of Pennsylvania, Philadelphia, PA19104-6272, USA.

0953-8984/91/479259 + 12 $03.50

For π-conjugated polymers such as polyacetylene and poly(para-phenylene vinylene), addition of charge (either electrons or holes) results in local geometrical relaxation of the chain in the vicinity of the charge, and these self-localized states are described as solitons, polarons or bipolarons. The geometrical relaxation of the chain moves states into the semiconductor gap, and these gap states give rise to sub-band-gap optical absorption. In the solid state, photoexcitation provides a means of creating these charged self-localized states, and also neutral excitations (excitons). Singlet excitons may decay radiatively to produce luminescence, and triplet excitons are most readily detected through a triplet–triplet induced absorption [9]. In the case where the excitations possess a net electrical charge, requiring separation of electrons and holes, photoconductivity and photoinduced absorption can be observed [10, 11].

In this paper we address the question of the formation and the behaviour of photoexcited states, both neutral and charged. We make comparison with the behaviour of conjugated polymers. We also discuss the effects of different amounts of C_{70} in the films of C_{60} on the response to photoexcitation.

2. Experimental procedure

Two different batches of samples were prepared. For both, graphite rods were evaporated in an arch discharge in 300 Torr helium and C_{60}/C_{70} was extracted from the 'soot' by Soxhlet extraction [5], yielding fullerene. This initial mixture was composed of about 70% C_{60} and 30% C_{70}. Finally, high-pressure liquid chromatography using 5% toluene in hexanes on neutral alumina [12] gave C_{60} of purity better than 99.9%; any residual traces of solvent were removed by vacuum drying overnight at 200 °C. Film deposition was performed in a standard evaporator (base pressure 10^{-7} Torr) using tungsten or molybdenum boats. Films grown from the purified source material contained less than 0.1% C_{70} and those from the unpurified C_{60}/C_{70} mixture had less than 10% C_{70}, as C_{60} is more volatile in the evaporation. Mass spectroscopy was used to check the content of C_{60} and C_{70}, and x-ray diffraction showed that C_{70} does not form a separate phase in the C_{60}, but is uniformly dispersed. We refer to these two batches of sample as C_{60} for those with less than 0.1% C_{70}, and as C_{60}/C_{70} for those with the higher C_{70} content.

We used films of thicknesses 0.1 μm (which appeared yellow/brown) and 1 μm (which appeared dark brown); both were deposited on silica substrates. The optical transmission spectra are presented as $\log(T_0/T)$, with T_0 the transmission of the substrate and T the measured transmission of the substrate with sample. We did not make corrections for reflectivity.

Measurements of dark conductivity and photoconductivity were made with both thick and thin films deposited on quartz substrates with an interdigitated array of gold electrodes (electrode spacing, 7 μm; electrode width, 300 mm). Measurements were carried out with a Keithley 617 electrometer, with temperature control provided by an Oxford Instruments He flow cryostat. The gold electrodes were found to provide ohmic contact to the films. As excitation source for the photoconductivity we used different lines of an argon-ion laser (UV or visible) or light of a 150 W tungsten lamp passed through a 1/4 m single monochromator. Samples were illuminated through the quartz substrate so that most of the pump light would be absorbed close to the electrodes for efficient collection of the excited charge carriers.

Spectrally resolved electroabsorption was measured on thin films on Spectrosil (silica glass) with interdigitated electrodes (0.2 mm electrode spacing and 60 mm electrode

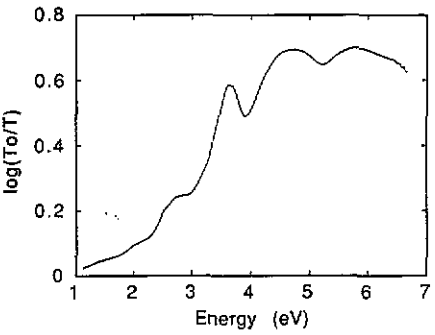

Figure 1. Optical absorption of a thin film of C_{60}/C_{70} at room temperature, measured as $\log(T_0/T)$.

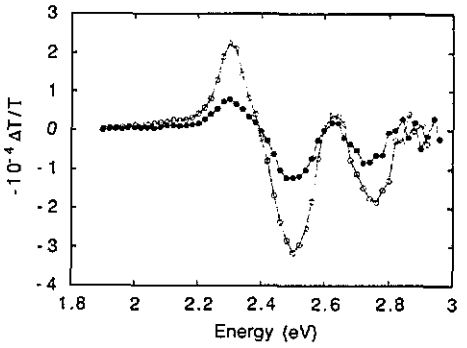

Figure 2. Normalized electroabsorption of a thin film of C_{60}; field strength of 55 kV cm^{-1}, $T = 80$ K; light polarization parallel (open circles) and perpendicular (full circles) to the direction of the applied electric field.

width). The spectra were recorded at liquid nitrogen temperature with applied electric fields of usually 55 kV cm^{-1} and light polarization parallel and perpendicular to the direction of the electric field. Luminescence was measured on thin samples with a double-grating monchromator with a Hamamatsu R943-02 photomultiplier tube. Different sample temperatures and excitation energies (UV and visible lines of an argon-ion laser) were used and the incident pump intensity was of the order of 1 W cm^{-2}. Photoinduced absorption was measured on both thin and thick samples on Spectrosil with the different lines of an argon-ion laser (mostly 457.9 nm, but also UV lines centred around 350 nm) as pump, and monochromatic light from a tungsten lamp as probe source. During these experiments the sample was kept at about or below 10 K in a He flow cryostat and we measured the spectral range from 500 to 2500 nm with Si, Ge and InAs detectors.

For all photoexcitation experiments the samples were maintained *in vacuo* and we kept the excitation intensities as low as possible, in order to limit possible thermal effects and sample degradation. In some of our experiments, when we used the UV lines of the argon laser as pump source, we saw indications of sample degradation as we discuss in sections 4 and 5, and observed that the C_{60}/C_{70} samples were more readily degraded than the C_{60} samples. Exposure of the samples to visible light even at elevated intensities did not have any observable effects, unless the vacuum was not very good or the samples were in some contact to moist atmosphere. Samples were stored in a dry nitrogen atmosphere in the dark, but were exposed to air during transport and whilst being mounted for experiments.

3. Results

3.1. Optical absorption and electroabsorption

Figure 1 shows the optical absorption (presented as $\log(T_0/T)$) of a thin film of C_{60}/C_{70} at room temperature. The spectra of the samples of C_{60} look very similar, even in the second derivative with respect to phonon energy which shows fine structure in the absorption edge much more clearly. The spectrum agrees well with spectra reported in

the literature [5, 13–18]. Since interactions between adjacent C_{60} molecules in the bulk are weak (Van- der- Waals interactions) [18–29] the structured absorption is well preserved as compared to the absorption in dilute solutions and thinner films [5, 13, 16, 30, 31]. However, there is a very clear indication of solid-state effects, in the form of peak broadening and stronger tailing in the solid state [5, 16, 17]. We see strong absorptions at about 3.63, 4.715 and 5.78 eV and a very extended structured tail to lower energies with a broad structured bump between 2.3 and 2.9 eV [5, 13, 16, 17, 30, 31]. Optical absorption measured in a thick film of C_{60}/C_{70} shows a sharp onset of absorption at 1.7 eV and marked Fabry–Ferot fringes below this absorption edge. (From these interference fringes and the measured film thickness, we calculate a refractive index of about 2.35 for the spectral range from 0.8 eV to 1.7 eV.) We have also calculated first and second (energy) derivatives of the absorption and measured the spectra also at $\simeq$80 K to obtain information about changes of the absorption with temperature (see below).

The three strong peaks in the optical absorption spectra seem to agree well with calculated spectra [14, 18]. The broad structured absorption between 2.3 and 2.9 eV in figure 1 is assigned to weakly allowed optical transitions including vibrational fine structure, and the behaviour at lower energies which is now well resolved in photothermal spectroscopy measurements, and can be characterized as an Urbach tail extending from 1.98 eV into the IR [17, 32]. In the region where the absorption is due to weakly allowed transitions, it is possible to obtain more information about these transitions by breaking symmetry, e.g. by measuring the change in optical absorption upon applied electric field (electroabsorption). Figure 2 shows polarized electroabsorption spectra of C_{60} at 80 K and field strength of 55 kV cm^{-1} with light polarization parallel and perpendicular to the direction of the applied electric field. An anisotropy of between 2.5 and 2.75 (for the different peaks in the spectrum) is observed with respect to the light polarization. The polarization dependence follows a $\cos^2$ law, and the response is quadratic in the applied electric field.

From our optical absorption measurements at room temperature and $\simeq$80 K, we have calculated the thermal modulation of the absorption of the C_{60} films. This spectrum is shown in figure 3. As in the second derivative with respect to energy of the absorption spectrum (now shown), we see that these are features near the strong optical absorptions.

3.2. Photoinduced absorption

We show in figure 4 the photoinduced absorption spectrum taken from a C_{60} sample at 67 Hz chop frequency, $T \simeq 10$ K, and 457.9 nm (2.7 eV) excitation wavelength at less than 50 mW cm^{-2}. Under these conditions the sample shows no degradation with time. This spectrum, which was obtained reproducibly for fresh samples, shows a broad double-peak structure between 1 and 2 eV. It was found to have a similar form for all pump wavelengths used (visible and UV argon laser lines). After prolonged exposure to UV light and, in particular, when we exposed the illuminated samples to a low pressure of air, a peak at 2.33 eV clearly emerged. We see this peak also for the C_{60}/C_{70} samples and note that it has been observed by other groups [32].

We measured the chop frequency, pump intensity and temperature dependence of the photoinduced absorption at 750 and at 1000 nm. The frequency dependence of the detection system response was carefully corrected, and for both wavelengths we did not observe a change of the signal strength within our experimental error from 9 Hz to above 3 kHz. This indicates that the lifetime of the excited states is less than 0.33 ms, in

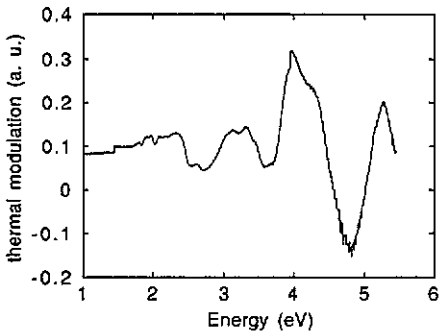

Figure 3. Thermal modulation of the optical absorption of a thin film of C_{60}/C_{70} measured as $-(T(300\,K) - T(80\,K))/T(300\,K)$; the discontinuities at 1.43 and 3.95 eV and the positive offset are due to the spectrometer.

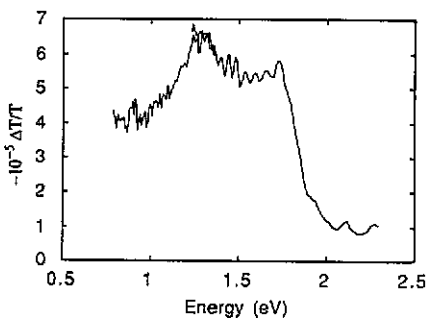

Figure 4. Normalized photoinduced absorption of a thin film of C_{60}; pump energy of 2.7 eV, pump intensity less than 50 mW cm^{-2}, 67 Hz chop frequency, $T \simeq 10$ K.

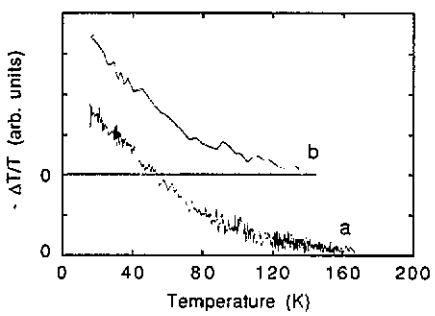

Figure 5. Temperature dependence of the photoinduced absorption of C_{60} for probe wavelengths of (a) 750 nm and (b) 1000 nm (curve (b) is displaced for clarity)—other parameters as in figure 4.

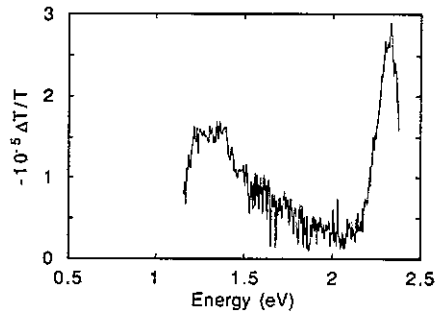

Figure 6. Normalized photoinduced absorption of a thin film of C_{60}/C_{70}; pump energy $\simeq$3.5 eV, pump intensity less than 15 mW cm^{-2}, 67 Hz chop frequency, $T \simeq 10$ K.

agreement with reported results for the lifetime of triplet states, but in disagreement with other measurements of photoinduced absorption [32]. The dependence of the signal upon the pump intensity was linear at both wavelengths up to the maximum pump intensities used. Figures 5(*a*) and (*b*) show the temperature dependence of the signals at 750 nm and 1000 nm respectively. The fall in signal with rising temperature is similar for the two wavelengths and the signals fall below the noise level above 120 K.

The spectrum for the thermal modulation of the absorption of the C_{60} films is shown in figure 3. There are features near the strong optical absorptions (see figure 1). Regarding the strength and the spectral shape of the thermal modulation there are no peaks in figure 3 which can account for the main absorptions in figure 4. This gives good evidence that we can exclude contributions from thermal modulation of the sample in the measured photoinduced absorption spectra.

Figure 6 shows the normalized spectrum of the photoinduced absorption for the C_{60}/C_{70} samples at about 10 K, chop frequency of 67 Hz and a pump energy of $\simeq$3.5 eV (the

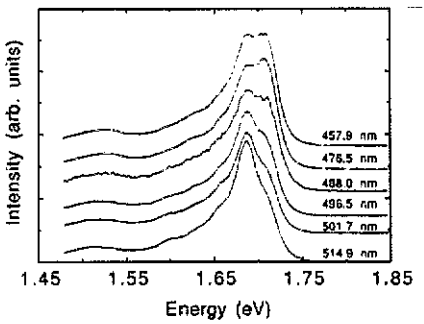

Figure 7. Photoluminescence of C_{60} at different excitation wavelengths (the spectra are displaced for clarity); incident pump intensity of the order of 1 W cm^{-2}; T = 78 K.

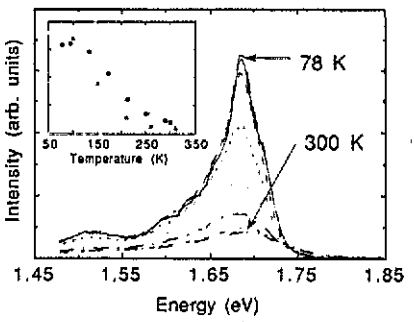

Figure 8. Photoluminescence of C_{60} at different temperatures from 78 to 300 K; the inset shows the temperature dependence of the main peak for C_{60} (circles) and C_{60}/C_{70} (triangles).

three argon laser UV lines) at less than 15 mW cm^{-2}. The spectrum is very different from that of the C_{60} samples. We observe two features; a narrow band at 2.33 eV (as found in degraded C_{60}), and a very broad asymmetric band with the maximum at about 1.3 eV. We also checked the spectral range from 1.1 eV to below 0.5 eV and, apart from the onset to the broad peak at 1.3 eV, did not see any signal above our noise level. The strength of the band at 2.33 eV was found to vary from sample to sample, though its shape and peak energy were found to be invariant. The shape and height of the broad peak around 1.3 eV was less reproducible; being significantly narrower in some samples than as shown in figure 6. We noticed some sample degradation and loss of signal intensity when using UV light as pump source, and found that the 1.3 eV feature was more affected by sample degradation than the 2.33 eV photoinduced absorption. Referring to figures 4 and 6, we note that we do not set great reliance on the relative signal strengths, as it is very difficult to determine experimentally the pump power actually absorbed in the samples.

3.3. Photoluminescence

Photoluminescence in C_{60} and/or C_{70} is seen at low temperatures in solutions [12] and in the solid state [16, 32]. We contrast here the results obtained for the C_{60} and C_{60}/C_{70} samples [33]. Figure 7 shows a series of photoluminescence spectra from the C_{60} sample at different excitation energies. The main peak is observed at 1.688 eV with a strong high-energy shoulder at 1.71 eV emerging at higher excitation energies. The shape of the peak in the samples with the higher C_{70} content does not change with excitation energy and the position is 1.713 eV (not shown). We attribute the differences in the C_{60} and C_{60}/C_{70} photoluminescence spectra and the excitation energy dependence to the different C_{70} content in these samples [33]. The vibrational sidebands of the luminescence [16, 33] are in good agreement with experimental and theoretical work on Raman spectroscopy [13, 16, 26, 33–35].

Figure 8 shows a series of luminescence spectra on the pure C_{60} at temperatures from 78 to 300 K and the inset shows the temperature dependences of the main peaks of the C_{60} and the C_{60}/C_{70} sample series. The signal decreases strongly with increasing

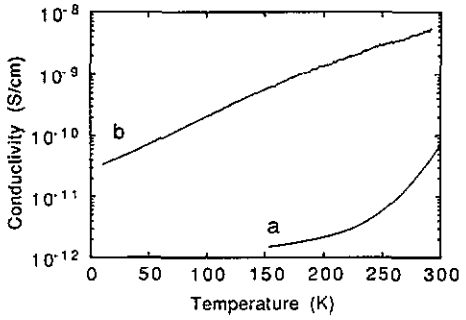

Figure 9. Dark conductivities of C_{60} (a) and C_{60}/C_{70} (b); measurable currents were limited to temperatures above 150 K.

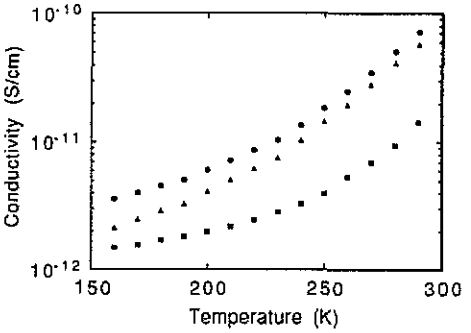

Figure 10. Dark conductivity, σ_{dark} (squares), conductivity under illumination (less than 3 mW cm^{-2} at 700 nm), σ_{total} (circles), and the photoconductivity, $\sigma_{photo} = \sigma_{total} - \sigma_{dark}$ (triangles) for C_{60}.

temperature from 100 to 300 K. Peak shifts with changing temperature are discussed elsewhere [33]. The vibrational sidebands of the luminescence are washed out and the low-energy tail broadens at higher temperatures. It is generally observed that vibrational structure in either the absorption edge or luminescence becomes more pronounced as the temperature is decreased.

3.4. Dark conductivity

Measurements were performed on both thin and thick films of C_{60} and C_{60}/C_{70} on arrays of interdigitated electrodes as a function of temperature. The behaviour of the C_{60} (and C_{60}/C_{70}) in our structures was found to be ohmic, indicating that gold is a satisfactory choice of contact material. Dark conductivities showed some variation from one sample to the other, with typical values of the order of 1×10^{-10} S cm^{-1} at room temperature; with the pure C_{60} samples showing lower values than the C_{60}/C_{70} samples. This value is significantly lower than the value of 10^{-5} S cm^{-1} reported by Haddon *et al* [36], but higher than the value of 10^{-14} S cm^{-1} recently reported by Mort *et al* [37].

We show the dark conductivity as a function of temperature for C_{60} in figure 9(*a*). The conductivity decreases only slowly as the temperature is lowered, and this weak temperature dependence is not satisfactorily fitted to standard transport models, such as activated behaviour or variable-range hopping. From the Arhennius plot ($\ln(\rho)$ against $1/T$), we calculate an activation energy of $\approx$0.43 eV for temperatures above $\approx$275 K, though the plot over the whole measured temperature range is not linear. This activation energy of 0.43 eV has to be regarded as a rough guide but is of a comparable energy scale to that of the optical absorption.

The dark conductivity of the C_{60}/C_{70} samples is shown in figure 9(*b*). The temperature dependence is significantly weaker than that of the C_{60} and an Arrhenius plot gives values for the activation energy of the order of 10 meV in the temperature range from 300 K to 10 K. Such values are very much smaller than the semiconductor gap.

We consider that the dark conductivity is probably due to a small concentration of extrinsic charge carriers, and that the weak temperature dependence arises from the temperature dependence of the mobility of these carriers. The decrease in mobility with

falling temperature is likely to arise from localization of the carriers due to disorder and/or impurities; this should be easily achieved in a system with weak intermolecular interactions. Evidence for the effects of disorder has been obtained from the form of the optical absorption in solid films, which shows a strong and very extended tail [17, 32]. We consider that the stronger temperature dependence of the conductivity in the C_{60} samples is closer to the intrinsic behaviour than that of the C_{60}/C_{70} samples.

3.5. Photoconductivity

Figure 10 shows the temperature dependence of the total conductivity under illumination, σ_{total}, the dark conductivity of C_{60}, σ_{dark}, and the difference between the two, $\sigma_{photo} = \sigma_{total} - \sigma_{dark}$. For this experiment excitation was at 700 nm (1.77 eV), provided by a 150 W tungsten lamp monochromated through a single monochromator with 2 mm slits, and glass high-pass filters, to give an excitation intensity of less than 0.15 mW on the whole sample ($\simeq$5 mm^2). Of interest here is the difference in the temperature dependence of σ_{dark} and σ_{photo}; it is clear from the figure that the photocurrent shows a considerably stronger temperature dependence than that due to the dark carriers. We have measured the photoresponse using excitation from the tungsten lamp from 350 nm up to above 2000 nm and, at all wavelengths, photoconductivity was observable, consistent with the absorption tail which extends to low energies. Even at 2000 nm excitation, the resistance drops by a factor of 1.5 (for the sample in figure 10). The C_{60} films were sufficiently photosensitive to produce a clear response merely by exposing the samples to room light through the cryostat windows. This large photoresponse of solid films of pure C_{60} is of some interest.

For the photoconductivity experiments on the C_{60}/C_{70} samples (the same samples as those used for dark conductivity measurements), we have pumped them with laser light at 2.4 eV, 2.7 eV and 3.5 eV at intensities of a few mW cm^{-2}. We saw clear indication of photoconductivity at all excitation energies, with a drop in resistance of the films from dark to illuminated ranging from a few per cent up to a factor of 10, depending on the sample and the pump energy and intensity. Temperature effects were shown to be unimportant by comparison with the temperature-dependent dark conductivity through calculation of the temperature modulation necessary to produce the measured conductivity changes. Pumping fresh samples with UV light at elevated intensities of $\simeq$10 mW on a spot of about 5 mm^2, we observed decreases of resistances of up to a factor of 40. However, we found that these excitation conditions quickly degraded the samples and caused a rapid loss of the photoconductivity signal.

Our measurements of the photoconductivity are consistent with those reported very recently by Mort *et al* [37]. They find a lower dark conductivity of 10^{-14} S cm^{-1} and relatively larger fractional changes in conductivity under illumination, by a factor of up to 10^2 at light intensities comparable to those used for the experiments on C_{60}, shown in figure 10. The excitation spectrum for the photoconductivity in our films clearly follows the optical absorption, with increasing photocurrent at higher pump energies, as found by Mort *et al* [37] for solid films and in correspondence with the results from electrochemical cells [38]. Our preliminary results on the pump intensity dependence of the photocurrent indicate that it quickly saturates when higher pump energies are used, even at the low pump intensities used with the monochromatized light from the tungsten lamp.

4. Discussion

We have presented a wide range of measurements of the effects of photoexcitation in C_{60} and we see that there is evidence for both charged excitations (photoconductivity) and neutral excitations (luminescence). We have also found that these states are created through excitation in the region of low absorption coefficient, below 3 eV, so first we discuss the nature of the optical transitions at these energies.

Both the electroabsorption (figure 2) and the thermal modulation (figure 3) spectra clearly reveal structure within this region of the absorption spectrum. The electroabsorption spectrum, for example, shows maxima at 2.30 and 2.63 eV and minima at 2.50 and 2.75 eV, and indications of further structure on a finer energy scale. Wei *et al* [32] have suggested that involvement of a phonon at about 750 cm^{-1} may fulfil the symmetry requirement for these otherwise forbidden transitions. We consider that it is important to examine further the role of symmetry breaking in this region of the absorption spectrum, and to examine other models. For example, it will be of interest to establish whether the electroabsorption matches the second derivative, with respect to energy, of the absorption spectrum, as is observed in conjugated polymers [39, 40]. In this case, the electroabsorption response can be described as a modulation of optically allowed transitions [41, 42]. Our measurements at present do not give sufficient information to resolve this issue.

Returning to the comparison with conjugated polymers, we note the similarities between the electroabsorption observed here and that measured in several of these polymers [39, 40]. Here, the signal is comparable to (but a little weaker than) the response observed in the polymers. By taking the frequency-dependent linear optical constants into account, the electroabsorption response can be related to non-linear optical coefficient, $\chi^{(3)}$ [39, 40], and this has been shown for the conjugated polymers to be generally very high. Hence, we expect the non-linear optical response of C_{60} (and C_{70}) to be relatively high, though the very broad absorption tail will reduce the figure of merit for applications in non-linear optics.

Photoluminescence provides direct evidence for the formation of neutral excited states, which, at low temperatures in C_{60}, is easily measured, indicating that there is therefore a relatively efficient radiative decay channel for the excited state. Wei *et al* [32] find that the lifetime is shorter than 3 μs and consider that the excited state is therefore a singlet, whereas Wasielewski *et al* [12] report a long-lived component with a lifetime of 53 ms. Our measurements, over a more limited frequency range, are in agreement with Wei *et al* [32]. We note that the photoluminescence shows a very strong temperature dependence. We consider that this is a clear indication of the importance of solid-state effects; the effect of increasing temperature being to allow channels for non-radiative decay to become effective, probably through increased mobility of the excitons and an increase in the rate of diffusion to non-radiative decay defect sites. Further investigation of this is required, including comparision of the temperature-dependent luminescence of isolated and condensed fullerene and consideration of the roles of other excited states present (those probed in the photoinduced absorption experiments).

Photoinduced absorption can arise from a wide range of excited states, both neutral and charged. Movement of oscillator strength into the gap can be achieved through relaxation of the excited-state geometry. In comparison to the quasi-one-dimensional conjugated polymers, C_{60}, with its shell structure, can be regarded as a two-dimensional π-system and hence geometrical relaxation in the excited states is not expected to be a

strong process, as the lattice energy of the two-dimensional cage will suppress such distortions [43]. However, creation of metastable triplet states via efficient inter-system crossing from photoexcited singlet states has been reported for both C_{60} and C_{70} in the gas phase [44], and in solution [12, 30, 31, 45, 46]. The lifetime of the triplet state measured in the different experiments varies from about 40 to more than 400 μs, but we can expect that the decay rate will be very dependent on the possibilities for decay through migration of triplets to allow annihilation at defect sites or through triplet–triplet collisions, and we expect that decay in solid films is more rapid than in the gas phase or in solution. The solution-phase measurements of Sension *et al* [31] show the build up of a photoinduced absorption band at 740 nm (1.67 eV) assigned to a triplet–triplet transition with a time constant of 0.65 ns. A similar result has been reported by Ebbesen *et al* [30].

We have found that the response at 750 and 1000 nm is due to states with lifetimes shorter than 0.33 ms, i.e. the response is fast in comparison with the chop frequency of the pump laser. We note that in this limit, the strength of the measured induced absorption scales with the lifetime of the excited states. Thus, we expect to see induced absorption due to triplet excitons, but not due to the short-lived singlet excitons. We assign the induced-absorption band in the C_{60} samples at 1.7 eV to the triplet–triplet transition identified in short-time measurements [30, 31]. As is evident in particular in figure 4, the signal does not go below zero, hence no bleaching was detectable in this spectral range. The origin of this overall positive background is not yet clear but has also been reported from the measurements in solution [30, 31] and in the solid state [32]. From the strong temperature dependence of the induced absorption (figure 5), we infer that the triplet lifetime falls rapidly with rising temperature.

In addition to the band at 1.7 eV, the induced absorption spectrum can show other features; for the C_{60} samples we have seen a band at 1.3 eV, and for the C_{60}/C_{70} samples, we see this and a band at 2.33 eV. The origin of these bands remains unclear at present, although our results indicate that there is, at the very least, some extrinsic stabilization of the states responsible for these absorption bands, particularly that at 2.33 eV. This extrinsic stabilization may arise through trapping of an intrinsic excited state of the C_{60} molecule at a defect site, so as to increase its lifetime (and hence the signal measured under our experimental conditions); C_{70} may fulfil this role. Alternatively, the excited state may bear little relation to any intrinsic molecular excitation; an example of this would be charge storage at a radical defect. We note that different kinetic behaviour of photoexcited states in C_{60} and C_{60}/C_{70} has been mentioned [31].

A source of long-lived excitation in the solid state can be the separation of electrons and holes to form positively and negatively charged species; in the case of the conjugated polymers, the lattice relaxation associated with polaron (or bipolaron) formation results in easily measured sub-gap absorption bands [10, 11]. This strong polaron formation taking place on the quasi-one-dimensional chains also slows down charge diffusion, so long lifetimes can be expected for these polymers even without extrinsic factors. Turning to C_{60}, we have established from the photoconductivity measurements that photo-excitation does lead to charge separation in the solid state. However, we consider that extrinsic factors are necessary to give rise to long-lived states because polaron formation is weak. We need to make comparison with experimental data for oxidized or reduced C_{60}. Kato *et al* [47] report that there are strong absorption bands due to the radical anion of C_{60} at 952 and 1076 nm (1.30 and 1.15 eV), and we consider that the induced-absorption band that we see in our samples at 1.3 eV may plausibly be attributed to such charged excitations. However, the band at 2.33 eV is not matched in the spectra due to Kato *et al*.

A further mechanism for the appearance of either absorption or bleaching bands in this experiment is through the photorefractive effect, in which charge separation leads to the setting up of local electric fields which modulate the optical absorption in the same way as achieved with an external field, as shown in figure 2. This has been observed in several conjugated polymers [48, 49]. The 2.33 eV peak in figure 6 coincides with the first positive feature of the electroabsorption in figure 2, but we do not see the full oscillatory response of the measured electroabsorption.

5. Conclusion

C_{60}, in the form of solid films, provides an interesting example of a molecular semiconductor in which intra-molecular and solid-state effects are both important. A further important factor is the role of disorder, defects and impurities (e.g. C_{70} in place of C_{60}). Our results are similar in many respects to those obtained from C_{60} in solution and which are therefore due to intra-molecular excitations. However, the clear evidence for photoseparation of electrons and holes in the photoconductivity measurements, and the presence of induced-absorption bands, which are not asigned to neutral excitations, indicates the role of intermolecular interactions in the solid state. Comparison with C_{60} which has charge introduced by other means will be of great interest, and we consider that the optical spectroscopy of field-induced charge layers in field-effect devices may provide useful information, as has been the case for conjugated polymers [50, 51].

Acknowledgments

The work in Cambridge was funded by the United Kingdom Science and Engineering Research Council. The work at the University of Pennsylvania was supported by the National Science Foundation Material Research Laboratory Program, DMR88-19885, and by the Department of Energy, DE-FC02.86ER45254.

References

[1] Curl R F and Smalley R E 1988 *Science* **242** 1017
[2] Kroto H W, Heath J R, O'Brien S C, Curl R F and Smalley R E 1985 *Nature* **318** 162
[3] Kroto H 1988 *Science* **242** 1139
[4] Krätschmer W, Fostiropoulos K and Huffman D R 1990 *Chem. Phys. Lett.* **170** 167
[5] Krätschmer W, Lamb L D, Fostiropoulos K and Huffman D R 1990 *Nature* **347** 354
[6] Rosseinsky M J, Ramirez A P, Glarum S H, Murphy D W, Haddon R C, Hebard A F, Palstra T T M, Kortan A R, Zahurak S M and Makhija A V 1991 *Phys. Rev. Lett.* **66** 2830
[7] Hebard A F, Rossiensky M J, Haddon R C, Murphy D W, Glarum S H, Palstra T T M, Ramirez A P and Kortan A R 1991 *Nature* **350** 600
[8] Miller J S 1991 *Adv. Mater.* **3** 262
[9] Colaneri N F, Bradley D D C, Friend R H, Burn P L, Holmes A B and Spangler C W 1990 *Phys. Rev.* B **42** 11670
[10] Friend R H, Bradley D D C and Townsend P D 1987 *J. Phys. D: Appl. Phys.* **20** 1367
[11] Heeger A J, Kivelson S, Schrieffer J R and Su W P 1988 *Rev. Mod. Phys.* **60** 782
[12] Wasielewski M R, O'Neil M P, Lykke K R, Pellin M J and Gruen D M 1991 *J. Am. Chem. Soc.* **113** 2774
[13] Ajie H, Alvarez M M, Anz S J, Beck R D, Diederich F, Fostiropoulos K, Huffman D R, Krätschmer W, Rubin Y, Schriver K E, Sensharma D and Whetten R L 1990 *J. Phys. Chem.* **94** 8634
[14] Larsson S, Volosov A and Rosen A 1987 *Chem. Phys. Lett.* **137** 501

[15] Hansen P L, Fallon P J and Krätschmer W 1991 *Chem. Phys. Lett.* **181** 367
[16] Reber C, Yee L, McKiernan J, Zink J I, Williams R S, Tong W M, Ohlberg D A A, Whetten R L and Diederich F 1991 *J. Phys. Chem.* **95** 2127
[17] Skumanich A 1991 *Chem. Phys. Lett.* **182** 486
[18] Saito S and Oshiyama A 1991 *Phys. Rev. Lett.* **66** 2637
[19] Zhang Q-M, Yi J-Y and Bernholc J 1991 *Phys. Rev. Lett.* **66** 2633
[20] Yannoni C S, Johnson R D, Meijer G, Bethune D S and Salem J R 1991 *J. Phys. Chem.* **95** 9
[21] Tycko R, Haddon R C, Dabbagh G, Glarum S H, Douglas D C and Mujsce A C 1991 *J. Phys. Chem.* **95** 518
[22] Saito Y, Shinohara H and Ohshita A 1991 *Japan J. Appl. Phys.* **30** L1068
[23] Terminello L J, Shuh D K, Himpsel F J, Lapiano-Smith D A, Stöhr J, Bethune D S and Meijer G 1991 *Chem. Phys. Lett.* **182** 491
[24] Lichtenberger D L, Nebesny K N, Ray C D, Huffman D R and Lamb L D 1991 *Chem. Phys. Lett.* **176** 203
[25] Jost M B, Troullier N, Poirier D M, Martins J L, Weaver J H, Chibante L P F and Smalley R E 1991 *Phys. Rev.* B **44** 1966
[26] Garrell R L, Herne T M, Szafranski C A, Diederich F, Ettl F and Whetten R L 1991 *J. Am. Chem. Soc.* **113** 6302
[27] Duclos S J, Brister K, Haddon R C, Kortan A R and Thiel F A 1991 *Nature* **351** 380
[28] Fischer J E, Heiney P A, McGhie A R, Romanow W J, Denenstein A M, McCauley J P and Smith A B III 1991 *Science* **252** 1288
[29] Benning P J, Poirier D M, Troullier N, Martins J L, Weaver J H, Hauffler R E, Chibante L P F and Smalley R E 1991 *Phys. Rev.* B **44** 1962
[30] Ebbesen T W, Tanigaki K and Kuroshima S 1991 *Chem. Phys. Lett.* **181** 501
[31] Sension R J, Phillips C M, Szarka A Z, Romanow W J, McGhie A R, McCauley J P, Smith A B III and Hochstrasser R M 1991 *J. Phys. Chem.* **95** 6075
[32] Wei X, Viner J, Vardeny Z V, Moses D, Srdanov V I and Wudl F 1991 *Synth. Met.* at press
[33] Graham S C, Pichler K, Friend R H, Romanov W J, McCauley J P, Coustel N, Fischer J E and Smith A B III 1991 *Synth. Met.* at press
[34] Bethune D S, Meijer G, Tang W C and Rosen H J 1990 *Chem. Phys. Lett.* **174** 219
[35] Negri F, Orlandi G and Zerbetto F 1988 *Chem. Phys. Lett.* **144** 31
[36] Haddon R C, Hebard A F, Rosseinsky M J, Murphy D W, Duclos S J, Lyons K B, Miller B, Rosamilia J M, Fleming R M, Kortan A R, Glarum S H, Makhija A V, Muller A J, Eick R H, Zahurak S M, Tycko R, Dabbagh G and Thiel F A 1991 *Nature* **350** 320
[37] Mort J, Okumura K, Machonkin M, Ziola R, Huffman D R and Ferguson M I 1991 *Chem. Phys. Lett.* at press
[38] Miller B, Rosamilia J M, Dabbagh G, Tycko R, Haddon R C, Muller A J, Wilson W, Murphy D W and Hebbard A F 1991 *J. Am. Chem. Soc.* **113** 6291
[39] Phillips S D, Worland R, Yu G, Hagler T, Freedman R, Cao Y, Yoon V, Chiang J, Walker W C and Heeger A J 1989 *Phys. Rev.* B **40** 9751
[40] Gelsen O M, Bradley D D C, Murata H, Tsutsui T, Saito S, Rühe J and Wegner G 1991 *Synth. Met.* **41–43** 875
[41] Keldysh L V 1958 *Sov. Phys.–JETP* **35** 1138
[42] Franz W 1958 *Z. Naturf.* **13** 484
[43] Hayden G W and Mele E J 1987 *Phys. Rev.* B **36** 5010
[44] Haufler R E, Wang L-S, Chibante L P F, Jin C, Conceicao J, Chai Y and Smalley R E 1991 *Chem. Phys. Lett.* **179** 449
[45] Arbogast J W, Darmanyan A P, Foote C S, Rubin Y, Diederich F, Alvarez M M, Anz S J and Whetten R L 1991 *J. Phys. Chem.* **95** 11
[46] Krusic P J, Wasserman E, Parkinson B A, Malone B, Holler J, Keizer E R P N, Morton J R and Preston K F 1991 *J. Am. Chem. Soc.* **113** 6274
[47] Kato T, Kodama T, Shida T, Nakagawa T, Matsui Y, Suzuki S, Shiromaru H, Yamauchi K and Achiba Y 1991 *Chem. Phys. Lett.* **180** 446
[48] Orenstein J, Baker G L and Vardeny Z 1983 *J. Physique Coll.* **44** C3 407
[49] Brassett A J, Colaneri N F, Bradley D D C, Lawrence R A, Friend R H, Murata H, Tokito S, Tsutsui T and Saito S 1990 *Phys. Rev.* B **41** 10586
[50] Burroughes J H, Jones C A and Friend R H 1988 *Nature* **335** 137
[51] Ziemelis K E, Hussain A T, Bradley D D C, Friend R H, Rühe J and Wegner G 1991 *Phys. Rev. Lett.* **66** 2231